MR and CT of Tuberous Sclerosis: Linear Abnormalities in the Cerebral White Matter

Satoru Iwasaki[1]
Hiroyuki Nakagawa[1]
Kimihiko Kichikawa[1]
Akio Fukusumi[1]
Yasuharu Watabe[1]
Kouji Kitamura[1]
Hideaki Otsuji[1]
Hajime Ohishi[2]
Hideo Uchida[1]

A review of MR and CT images in five patients, 8 months to 22 years old, diagnosed as having tuberous sclerosis, revealed linear abnormalities in the cerebral white matter. A linear abnormality connecting a subependymal nodule to a subcortical lesion was shown in two patients as an area of hypointensity on T1-weighted MR images and as an area of hyperintensity on T2-weighted images. These appeared as faintly high-density areas on CT images. Seventeen linear abnormalities extending from the ventricle to the cortex with a subependymal nodule or subcortical lesion on each end were visible in all five patients as areas of hyperintensity on the T2-weighted images. On the T1-weighted images, only nine hypointense lines were noted. CT scans did not show these latter lines.

Linear abnormalities in cerebral white matter are suggestive of lesions of demyelination, dysmyelination, hypomyelination, or lines of migration disorder. MR imaging, especially T2-weighted, is particularly sensitive in detecting these abnormalities.

***AJNR* 11:1029–1034, September/October 1990**

The noninvasive diagnosis of tuberous sclerosis is possible by CT because this imaging technique shows a subependymal nodule as a focus of calcification or as a nodular structure, and it shows an abnormality of the cerebral white matter as a low-density area or a calcification [1–4]. In addition, CT detects tumors at early stages of growth [5, 6].

With MR, it is not only possible to visualize a subependymal nodule and lesions of white matter but also cortical tubers, which are difficult to identify by CT. For this reason, MR is more sensitive than CT in diagnosing tuberous sclerosis [7–11]. We have recently detected linear abnormalities that connect the ventricle to the cerebral surface. We describe this finding in MR and CT images.

Subjects and Methods

Five subjects, two males and three females, 8 months to 22 years old, were studied prospectively. Seizures were found in all patients. Case 1 had depigmentation of the hip; the other four patients had sebaceous adenoma of the face. Mental retardation was found in all but one patient. Case 5 had angiomyolipomas in both kidneys.

MR imaging was performed on a 1.5-T unit (Vista, Picker International, Inc., Highland Heights, OH). T1-weighted images were obtained by inversion recovery, 2000–2500/30/600/1, or 2000/30/150/1 (TR/TE/TI/excitation). T2-weighted images were obtained by spin-echo technique (1500–2000/100/2). Sixteen serial 7-mm-thick sections were acquired with no interslice gap. The matrix size used for reconstruction was 192 × 256. For T2-weighted images, a motion artifact suppression technique (MAST) [12] was used in all but case 5. T2-weighted imaging in case 2 was carried out with and without MAST.

Results

A moderate degree of atrophy was manifested in two of the five cases (Table 1 and Figs. 1 and 2). Subependymal nodules were seen on CT as foci of calcification

Received November 28, 1989; revision requested December 21, 1989; revision received February 21, 1990; accepted March 12, 1990.

Presented at the annual meeting of the Japanese Neuroradiological Society, Yamagata, February 1988.

[1] Department of Radiology, Nara Medical University, 840 Kashihara-shi, Nara 634, Japan. Address reprint requests to S. Iwasaki.

[2] Department of Oncoradiology, Nara Medical University, Nara 634, Japan.

0195-6108/90/1105-1029

TABLE 1: MR, CT, and Clinical Profiles of Five Patients with Tuberous Sclerosis

Case No.	Age	Sex	Clinical Findings	Atrophy on CT or MR	Number of Subependymal Nodules[a]		Number of Parenchymal and Cortical Lesions[a]	
					CT	MR	CT	MR
1	8 mo	F	Mental retardation, seizure, depigmentation of hip	Moderate	2 (2)	7	0	1
2	6 yr	F	Seizure, sebaceous adenoma	None	(3)	3	1	3
3	8 yr	M	Mental retardation, seizure, sebaceous adenoma	None	(10)	12	3	14
4	19 yr	F	Mental retardation, seizure, sebaceous adenoma	None	(8)	8	(8)	8
5	22 yr	M	Mental retardation, seizure, sebaceous adenoma, renal angiomyolipoma	Moderate	(11)	8[b]	(1)	Many

[a] Numbers in parentheses are calcified lesions.
[b] Including a tumor.

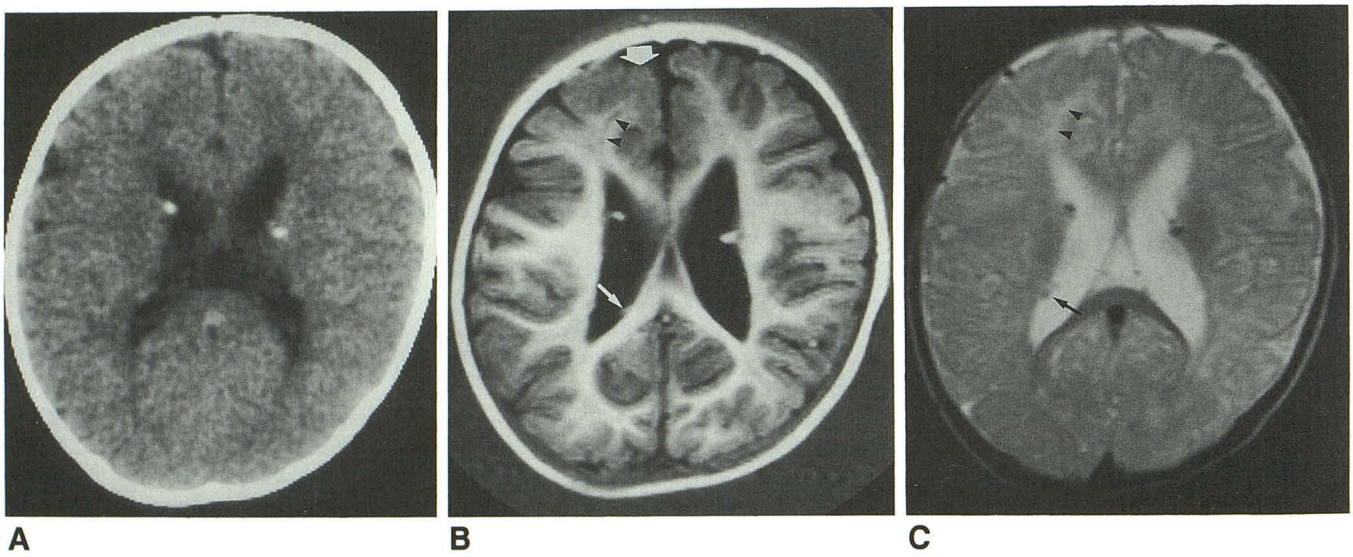

Fig. 1.—Case 1: 8-month-old-girl. Plain CT (*A*); T1-weighted MR image, IR 2500/30/600 (*B*); and T2-weighted MR image, SE 2000/100 with MAST (*C*). The calcified subependymal nodules demonstrated on CT (*A*) are seen with same signal intensity as white matter on T1-weighted MR image (*B*). These are seen as signal voids on T2-weighted MR image (*C*). Furthermore, a nodule (*thin arrow* in *B*) is visible medial to atrium of right lateral ventricle, and nodules of same signal intensity as gray matter (*arrow* in *C*) are visible at posterolateral aspect of right lateral ventricle. Branching of right superior frontal gyrus is reduced, suggesting formation of a cortical tuber (*wide arrow* in *B*). In the subcortical lesion corresponding to the area of suspected cortical tuber, a line is seen as a hypointense area on the T1-weighted image (*B*) and as an area of somewhat higher intensity than surrounding white matter on T2-weighted image (*C*). It reaches the ventricular wall (*arrowheads* in *B* and *C*), but a subependymal nodule is not detectable at the ventricular site.

or as noncalcified nodular structures. MR imaging showed these nodules as having the same signal intensity as white matter on the T1-weighted images and as signal voids on the T2-weighted images (Table 1 and Figs. 1–3).

In case 5, a tumor was detected at the right foramen of Monro only on the MR images. It was seen as a hypointense area on the T1-weighted sequence and as a hyperintense area on the T2-weighted sequence (Fig. 2). An abnormality of gray matter was detected in case 1 only as decreased branching of the right superior frontal gyrus (Fig. 1).

Lesions of the white matter were shown on CT as foci of calcification (Table 1 and Fig. 2) and as areas of low density (Table 1 and Fig. 3). The areas that appeared as calcification on CT scans were seen as signal voids on both the T1- and T2-weighted MR images (Fig. 2). Other white matter lesions were seen as hypointense structures on the T1-weighted images and as hyperintense structures on the T2-weighted images (Table 1 and Figs. 2 and 3).

A signal void was detected on the T1-weighted image at the left coronal suture in case 5 (Fig. 2). This could not be

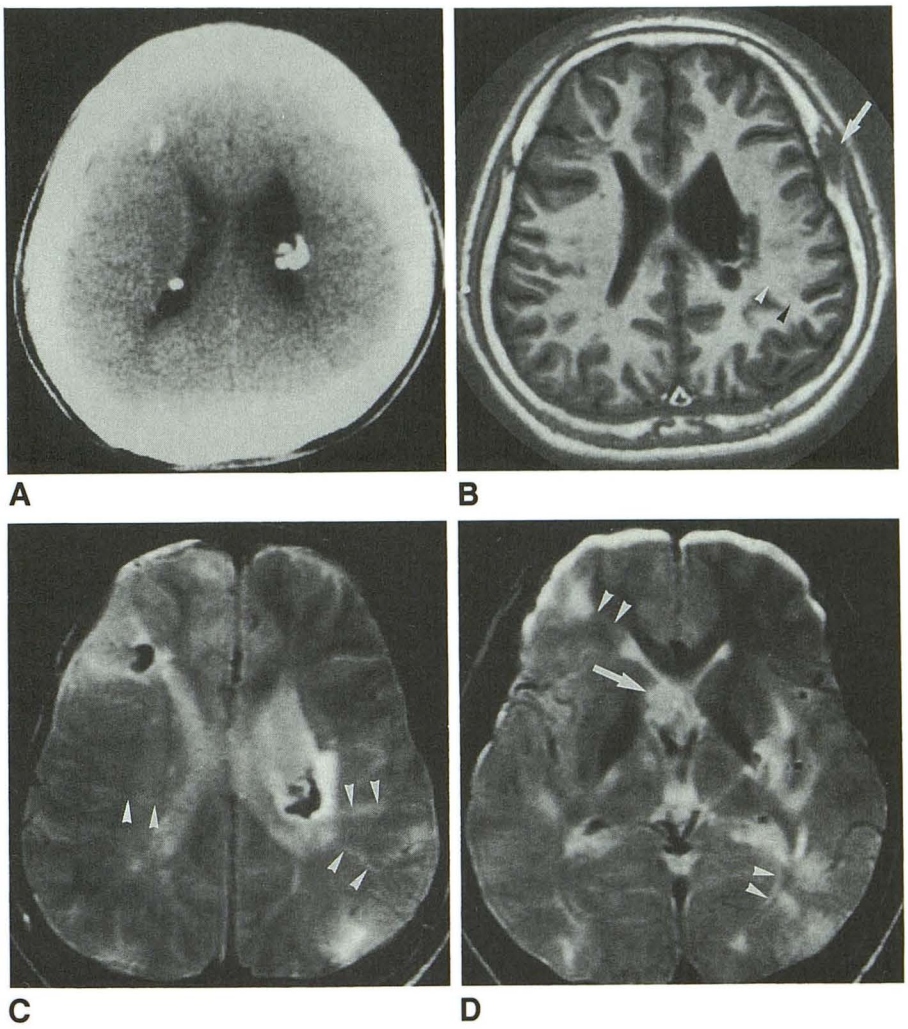

Fig. 2.—Case 5: 22-year-old man. Plain CT (*A*); T1-weighted MR image, IR 2000/30/600 (*B*); and T2-weighted MR images, SE 1500/100 without MAST (*C* and *D*). Hyperintense linear abnormalities (*arrowheads* in *C* and *D*) are seen between subependymal nodule and cortex (*C*), and between subcortical lesion and ventricular wall (*D*). One of them is also seen on T1-weighted MR image as an area of hypointensity (*arrowheads* in *B*). No linear abnormality is demonstrated on CT (*A*). A hyperintense tumor (*arrowhead* in *D*) is visible at right foramen of Monro. On T1-weighted image, an osteosclerotic lesion in area of left coronal suture is seen as a signal void (*arrow* in *B*).

detected by CT with a usual brain window width but was verified as a bony sclerosis when the window width was increased.

Linear abnormalities connecting a subependymal nodule to a cortical lesion were detected in two cases as areas of hypointensity on the T1-weighted images and as areas of hyperintensity on the T2-weighted images. These appeared as faint high-density areas (Hounsfield units of line/putamen: case 2 = 52/35; case 4 = 55/43) without enhancement on the CT image even after contrast infusion (case 2 = 57/44; case 4 = 58/47) (Table 2 and Fig. 3).

The linear abnormalities reaching the ventricular wall from the cortical lesions but lacking evidence of a nodule at the ventricular wall appeared as areas of hyperintensity on the T2-weighted images in four cases and as areas of hypointensity on the T1-weighted images in three cases. These were not seen on the CT scans (Table 2 and Figs. 1 and 2).

The linear abnormalities reaching the cortex from subependymal nodules but lacking evidence of a cortical lesion were detected as areas of hyperintensity on the T2-weighted images in four cases and as areas of hypointensity on the T1-weighted images in two cases. These were not visualized by CT (Table 2 and Figs. 2 and 3). The use of MAST in MR imaging did not further characterize the abnormalities.

Discussion

Tuberous sclerosis belongs to the group of diseases known as phacomatosis. Intracranial phacomatosis has been reported to include subependymal nodules, cortical tubers, subcortical demyelination, dysmyelination, hypomyelination, and clusters of heterotopic neuronal or glial cells [13–17].

CT can identify minimal calcification of a subependymal nodule or white matter lesion [1, 4, 5]. Demyelination or hypomyelination appears as a low-density structure [2, 13]. CT is, therefore, indispensable in the diagnosis of tuberous sclerosis.

MR imaging has been considered less effective than CT in identifying calcification of a subependymal nodule [8–11]. In the present experiment, it was difficult to confirm by MR whether a nodule was calcified or not. However, MR is more effective than CT in delineating details and detecting gyral tubers [7–11, 13]. In two of five cases, more subependymal nodules were identified by MR than CT. The signal intensity

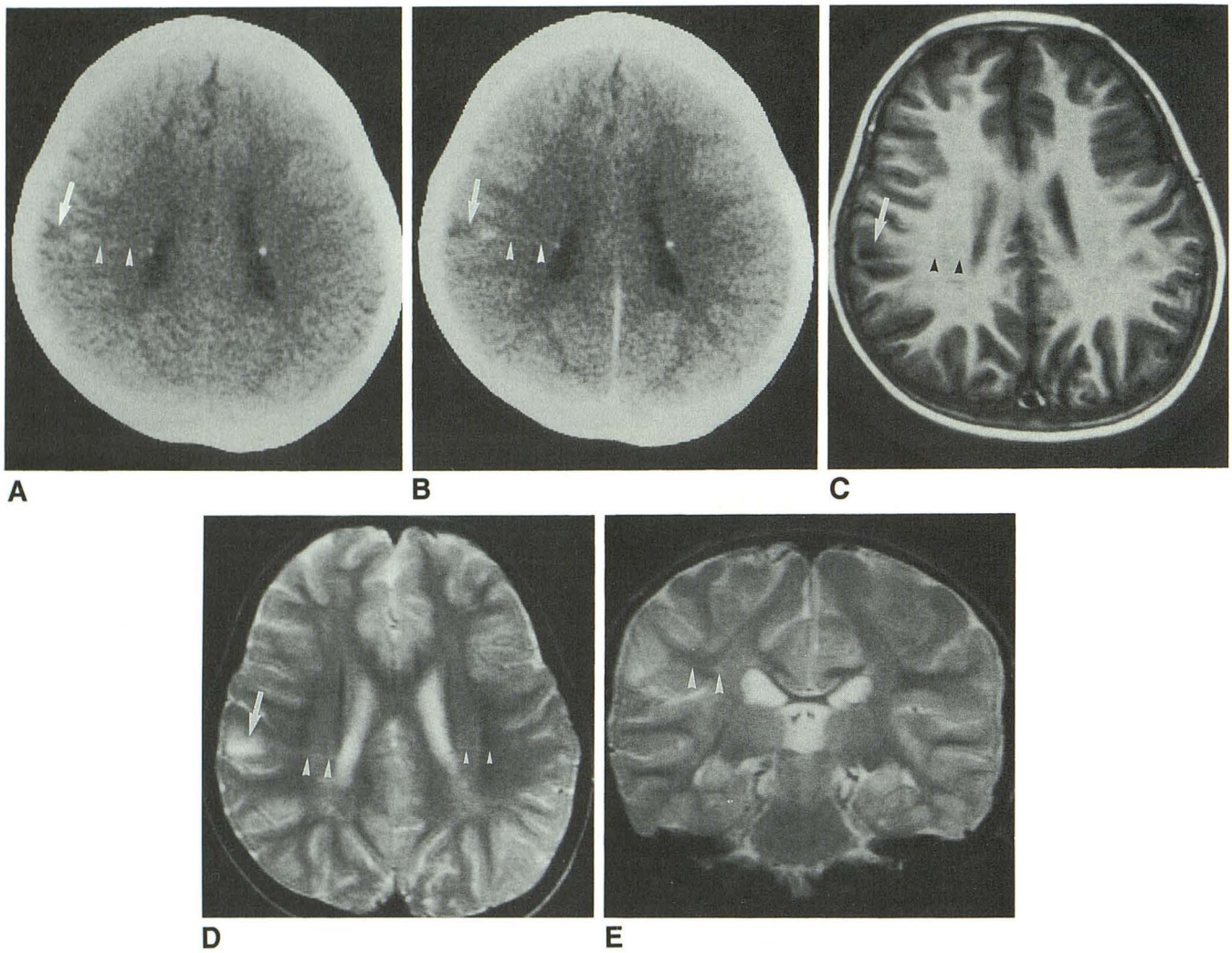

Fig. 3.—Case 2: 6-year-old girl. Plain (*A*) and enhanced (*B*) CT scans; T1-weighted MR image, IR 2500/30/600 (*C*); and transverse (*D*) and coronal (*E*) T2-weighted MR images, SE 2000/100 with MAST. A line (*arrowheads*) connecting subependymal nodule at right lateral ventricle to subcortical lesion (*arrow*) on supramarginal gyrus in seen as an area of faint high density on plain CT (*A*) without increase of density on contrast enhanced CT (*B*), as an area of hypointensity on T1-weighted MR image (*C*), and as an area of hyperintensity on T2-weighted MR images (*D* and *E*). A very faint hyperintense line (*small arrowhead* in *D*) appears to run from a small subependymal nodule in left lateral ventricle to the cortex, but evidence of subcortical lesion is not distinct.

of subependymal nodules was almost identical to white matter on the T1-weighted images (inversion recovery). They appeared as signal voids on the T2-weighted images. This confirmed the findings of Inoue et al. [10].

The parenchymal lesions, which were visualized by CT as calcified, were identified distinctly by MR as signal voids on both the T1- and T2-weighted images. The parenchymal lesions, which were not calcified on CT, were detected far more frequently by MR either as hypointense structures on the T1-weighted images or as hyperintense structures on the T2-weighted images.

In one case (Fig. 1), a cortical tuber was detected by MR as an abnormality of gyral branching. In other cases, cortical tubers were suggested by wedge-shaped subcortical areas of hypointensity on T1-weighted images and as areas of hyperintensity on the T2-weighted images (Figs. 2 and 3) [7, 10].

A number of linear abnormalities connecting the ventricular wall to the cerebral surface were detected in the white matter of these patients. The outline of these abnormalities may be divided into three patterns: (A) a linear abnormality with a subependymal nodule at one end and subcortical lesion at the other; (B) a linear abnormality with a subcortical lesion at one end but without a subependymal nodule adjacent to the ventricular wall; and (C) a linear abnormality with a subependymal nodule at one end but without a subcortical lesion at the cerebral surface (Table 2). MR delineated these three patterns of linear abnormalities as hypointense areas on the T1-weighted images and as hyperintense areas on the T2-weighted images.

TABLE 2: CT and MR Demonstration of Linear Abnormalities

Case	Number of Linear Abnormalities Connecting with. . .					
	Cortical Tubers and Subependymal Nodules		Cortical Tubers		Subependymal Nodules	
	T1	T2	T1	T2	T1	T2
1	—	—	1	1	—	—
2	1*	1*	—	—	—	1
3	—	—	1	1	2	3
4	1*	1*	—	1	—	1
5	—	—	4	5	1	4

Note.—T1 = T1-weighted image; T2 = T2-weighted image.
* = Visible on CT.

CT delineated the first pattern (A) as a faintly high-density area but failed to detect the second and third patterns (B and C). Although we preferred inversion recovery to a short TR/short TE spin-echo sequence, the latter was not used for T1-weighted images. T2-weighted MR imaging was found to be best for detecting these linear abnormalities.

Pattern A was detected in two cases. Both were found to connect the posterolateral region of the body of the right lateral ventricle to the supramarginal gyrus. The other linear patterns seemed to run either from the body of a lateral ventricle or from the anterior horn of a lateral ventricle to the superior or middle frontal gyrus. Such appearances suggest that only those linear abnormalities running in a horizontal direction and caught in the 7-mm thickness of the transverse section were visualized in the lines stemming from the lateral ventricle. Hence, linear abnormalities B and C have two possible explanations. The first is that the abnormalities do not have a subependymal nodule or subcortical lesion on each end; the second is that the abnormalities run oblique to the transverse section and are, therefore, delineated by a lack of either the upper or lower end, which contains a subcortical lesion or a subependymal nodule. The appearance of both cases of type (A) linear abnormalities on the right side may be due to the left-to-right asymmetry of the superior temporal gyrus and planum temporale [18].

Since the medullary veins show a similar pattern of arrangement, it is necessary to differentiate them from linear abnormalities. The linear abnormalities did not increase in density on enhanced CT scans. The MR images looked almost identical when examined with and without MAST. It is, therefore, unlikely that these abnormalities represent medullary veins [12].

Virchow-Robin spaces also should be considered in the differential diagnosis of linear abnormalities in white matter. Heier et al. [19] reported that the Virchow-Robin spaces increased in size and rate of occurrence with advancing age and that grade 1 spaces (under 2 mm in diameter, and including lenticulostriate spaces and high-convexity spaces) were seen in 23% of patients under age 20. The grade 2 and 3 high-convexity spaces (over 2 mm in diameter) had much stronger correlation with age and were not found in patients under age 29 [19]. In our patients, linear abnormalities were seen in the high-convexity spaces and not in the lenticulostriate areas. The lines in tuberous sclerosis were different from the Virchow-Robin space in having a subependymal nodule and/or cortical tuber (subcortical lesion) on each end. Although the frequency and morphology suggest that the lines are different from Virchow-Robin spaces, it is possible that some lines represent enlargement of Virchow-Robin spaces due to white matter lesions such as demyelination beneath the cortical tuber.

Since the linear abnormalities had the same signal intensity as demyelination and seemed to be joined by subcortical lesions at the cortical end in the MR images, these are likely to represent demyelination, dysmyelination, or hypomyelination. Nixon et al. [11] mentioned that deep periventricular white matter lesions on the T2-weighted images were probably in continuity with superficial lesions, which were suggested as hypomyelination from his autopsy study [13]. They did not illustrate the connection nor did they propose that it might reflect a migration disorder.

In the CT images, two lines had faintly high density. These trailed from the subependymal nodule to the subcortical lesion but the others were not visualized. Pinto-Lord et al. [3] reported a case of tuberous sclerosis with a high-density, wedge-shaped, nonenhanced lesion in the left parietal region extending from the ventricle to the pial surface on the CT image. Neuropathologic examination revealed findings consistent with a cortical tuber having a high content of calcium. The lines demonstrated on the CT images in our cases are similar to those seen by Pinto-Lord et al. except that the width is very narrow and there is a subcortical lesion on the pial end. If this is so, the lines may represent the lesion of a migrational disorder. Linear abnormalities as a new feature of tuberous sclerosis may become increasingly helpful for the diagnosis and clarification of the pathogenesis of this disease.

REFERENCES

1. Gomez MR, Mellinger JF, Reese DF. The use of computerized transaxial tomography in the diagnosis of tuberous sclerosis. *Mayo Clin Proc* **1975**;50:553–556
2. Garrick R, Gomez MR, Houser OW. Demyelination of the brain in tuberous sclerosis: computed tomography evidence. *Mayo Clin Proc* **1979**;54:685–689
3. Pinto-Lord MC, Abroms IF, Smith TW. Hyperdense cerebral lesion in childhood tuberous sclerosis: computed tomographic demonstration and neuropathologic analysis. *Pediatr Neurol* **1986**;2:245–248
4. Kingsley DPE, Kendall BE, Fitz CR. Tuberous sclerosis: a clinico-radiological evaluation of 110 cases with particular reference to atypical presentation. *Neuroradiology* **1986**;28:38–46
5. Barry JF, Harwood-Nash DC, Fitz CR, Byrd SE. Unrecognized atypical tuberous sclerosis diagnosed with CT. *Neuroradiology* **1977**;13:177–180
6. Winter J. Computed tomography in diagnosis of intracranial tumors versus tubers in tuberous sclerosis. *Acta Radiol [Diagn]* (Stockh) **1982**;23:337–344
7. Terwey B, Doose H. Tuberous sclerosis: magnetic imaging of the brain. *Neuropediatrics* **1987**;18:67–69
8. McMurdo SK Jr, Moore SG, Brant-Zawadzki M, et al. MR imaging of

intracranial tuberous sclerosis. *AJNR* **1987**;8:77–82
9. Roach ES, Williams DP, Laster DW. Magnetic resonance imaging in tuberous sclerosis. *Arch Neurol* **1987**;44:301–303
10. Inoue Y, Nakajima S, Fukuda T, et al. Magnetic resonance images of tuberous sclerosis: further observations and clinical correlations. *Neuroradiology* **1988**;30:379–384
11. Nixon JR, Houser OW, Gomez MR, Okazaki H. Cerebral tuberous sclerosis: MR imaging. *Radiology* **1989**;170:869–873
12. Pattany PM, Phillips JJ, Chiu LC, et al. Motion artifact suppression technique (MAST) for MR imaging. *J Comput Assist Tomogr* **1987**;11:369–377
13. Nixon JR, Miller GM, Okazaki H, Gomez MR. Cerebral tuberous sclerosis: postmortem magnetic resonance imaging and pathologic anatomy. *Mayo Clin Proc* **1989**;64:305–311
14. Larroche JC. Malformations of the nervous system. In: Adams JH, Corsellis JAN, Duchen LW, eds. *Greenfield's neuropathology*. London: Edward Arnold Ltd, **1984**:427–430
15. Haberland C. The phakomatoses. In: Vinken PJ, Bruyn GW, eds. *Handbook of clinical neurology*, vol 31. Amsterdam: North-Holland, **1977**:4–10
16. Trombley IK, Mirra SS. Ultrastructure of tuberous sclerosis: cortical tuber and subependymal tumor. *Ann Neurol* **1981**;9:174–181
17. Bender BL, Yunis EJ. The pathology of tuberous sclerosis. *Pathol Annu* **1982**;17:339–382
18. Iwasaki S, Kichikawa K, Nakagawa H, et al. Left-right asymmetry in the temporal and parietal region based on the medullary pattern of cerebral white matter. *Acta Radiol Suppl* (Stockh) **1986**;369:208–211
19. Heier LA, Bauer CJ, Schwartz L, Zimmerman RD, Morgello S, Deck MDF. Large Virchow-Robin spaces: MR-clinical correlation. *AJNR* **1989**;10:929–936